

# Optical Interference Coating Design Contest 2022: a black box coating and a filter for an outdoor 3D cinema challenge [invited]

JENNIFER D. T. KRUSCHWITZ,<sup>1,\*</sup>  MICHAEL TRUBETSKOV,<sup>2</sup>  AND JASON KECK<sup>3</sup>

<sup>1</sup>*Institute of Optics, University of Rochester, 480 Intercampus Drive, Rochester, New York 14627, USA*

<sup>2</sup>*Max Planck Institute of Quantum Optics, Hans-Kopfermann-Str., 85748 Garching, Germany*

<sup>3</sup>*Independent consultant, Pelham, New Hampshire 03076, USA*

\*Corresponding author: [jennifer.kruschwitz@rochester.edu](mailto:jennifer.kruschwitz@rochester.edu)

Received 5 September 2022; accepted 30 October 2022; posted 8 November 2022; published 15 December 2022

The design problems for the Optical Interference Coating (OIC) 2022 Topical Meeting include black box coatings to reverse engineer and a pair of white-balanced, multi-bandpass filters for three-dimensional cinema projection in cold and hot outdoor environments. There were 14 designers from China, France, Germany, Japan, Russia, and the United States, submitting 32 total designs for problems A and B. The design problems and the submitted solutions are described and evaluated. © 2022 Optica Publishing Group

<https://doi.org/10.1364/AO.474957>

## 1. INTRODUCTION

The design contest has been a staple of the Optical Interference Coating (OIC) Topical Meeting for nearly three decades. A design challenge was proposed in October 2021 to optical coating designers and the optical thin-film community across the globe. The use of any design software and design methods are encouraged with the goal of meeting the requirements within each specific design problem. Submitted designs are reviewed, analyzed, and ranked based on a definitive set of criteria. The top three designs submitted are awarded special recognition at the meeting. All designers are encouraged to accompany their designs with specific design methodology, which many times advances the global knowledge base of the optical interference coating community.

Submissions were received from 14 designers in six different countries: China, France, Germany, Japan, Russia, and the United States (see Table 1). In total, there were 32 submitted designs for the OIC 2022 Design Contest in Whistler, Canada. Issuing new design problems, even every three years, is no easy task for the Design Challenge Committee. It takes many months to come up with general concepts that the community will find interesting, yet not too difficult to find a solution. The concepts are tested by the committee to make sure that each has explicit requirements, and that they are engaging to all (especially those in the industry). The last, and most important, requirement is that they cannot be solved *easily* by modern design software. The final designs chosen for the OIC 2022 Design Challenge were a black-box coating and white-balancing, multi-bandpass filters.

The evaluation software for the 2022 contest was written in C# using the Blazor/.NET Core frameworks hosted on

**Table 1. Designers and Design Submissions for Problems A1, A2, B1, and/or B2**

Designer	Institution	A1	A2	B1	B2
Ilya Bolshakov	AOC Optex, USA	✓	–	–	–
Daniel Tchoonghyon Kim <sup>a</sup>	Viavi Solutions, USA	✓	✓	–	–
Fabien Lemarchand	Institut Fresnel, FRANCE	✓	✓	–	–
Bruce Perilloux	Coherent, Inc., USA	✓	–	–	–
Iurii Prosovskii and Oleg Prosovskii	RUSSIA	✓	✓	–	–
Javier Ruiz	Independent Consultant, USA	✓	–	✓	✓
William Southwell and Joseph Peeples	Table Mountain Optics, USA	✓	✓	–	–
Diana Tonova	Carl Zeiss, GERMANY	✓	✓	–	–
Wenjia Yuan	Zhejiang University, CHINA	✓	–	–	–
Sakurai Yuki	Ceratech, JAPAN	✓	✓	–	–
Jinlong Zhang and Xiaochuan Ji	Tongji University, CHINA	✓	✓	–	–

<sup>a</sup>Late submission.

an Ubuntu server running Apache. Calculations were performed on the server to ensure consistent results on different environments—due to different implementations and of floating point arithmetic, different machines may produce output with exceedingly small discrepancies. Using a single machine for calculation eliminates this potential source of confusion.

Post-production characterization of multilayer coatings (also known as reverse engineering, or re-engineering) is an important part of coating production. For successful post-production characterization, it is necessary to know the theoretical design, and

the goal of post-production characterization is to identify deviations in deposition conditions that contribute to the differences between measured spectral characteristics and theoretical ones.

From time to time, the designer may attempt to use multilayer design methods for performing post-production characterization without knowledge of the theoretical design or specifics about the manufacturing process. A question arises from this procedure: is it possible to reconstruct the exact theoretical design structure using reverse engineering of measured spectra?

To demonstrate how complicated (if even possible) the reconstruction of an unknown design is, we propose a Black Box Coating challenge. The number of layers, layer thicknesses, and the arrangement of layer materials are unknown in this challenge.

In Problem A, we propose two exercises of different complexities:

- Subproblem A.1: black box antireflection (AR) coating;
- Subproblem A.2: black box short-wavelength pass, non-polarizing filter (SWPNPF).

For subproblem A.1, we provide precomputed reflectance and transmittance spectra. For subproblem A.2, we provide an ability to perform arbitrary queries to obtain transmittance and reflectance spectra using a virtual, web-based spectrophotometer. The angle of incidence, light polarization, wavelength ranges, and wavelength increments can be configured within some permitted ranges. We do not add any measurement errors to reflectance or transmittance spectra, assuming ideally accurate measurements, which are never possible in practice.

Problem B involves enabling 3D cinema technology to be accessible during the pandemic for the designer and their family. The restrictions imposed on entertainment facilities due to COVID-19 have limited everyone's ability to enjoy 3D movies on a big screen. The designer's extended family are in different parts of the world, and all have grown very tired of gathering for "Movie Nights" through computers and watching 2D movies on their televisions. The solution will be to create an outdoor theater so that everyone can recapture the experience of watching 3D movies together without risking safety protocols due to the pandemic. Optical components such as polarizers are in very short supply. However, the designer has their own coating facility and access to eyewear frames and glass lenses. It is up to the designer to design a set of white-balanced, multi-bandpass filters that can be used in a pair of 3D cinema glasses. The filters will be identical in the projector and the eyewear. The projector filters will maintain a temperature of 20°C, while the temperature of the eyewear will change with the outdoor environment.

In Problem B, the two challenges include:

- Subproblem B.1: minimize color differences at a cold location in the world (indices for  $-50^{\circ}\text{C}$  are provided);
- Subproblem B.2: minimize color differences at a hot location in the world (indices for  $+50^{\circ}\text{C}$  are provided).

Both the cold and hot locations were announced with their outdoor temperatures at the OIC 2022 Topical Meeting.

## 2. PROBLEM A: A BLACK BOX COATING

For both subproblems, reflectance  $R$  and transmittance  $T$  data are provided without taking into account substrate backside reflections. Therefore, the substrate should be considered as a semi-infinite medium with a coating placed at the boundary between the substrate and incident medium with the refractive index 1.0. In this exercise, measurement errors, being the main limiting factor for post-production characterization of optical coatings, have been eliminated. Accurate data are provided for  $R$  and  $T$ , where the accuracy is limited only by very small round-off errors.

### A. Layer Materials and Substrate

For both Problem A1 and Problem A2, we consider a non-absorbing BK7 substrate with the refractive index given by the Sellmeier dispersion formula

$$n^2(\lambda) - 1 = \frac{B_1\lambda^2}{\lambda^2 - C_1} + \frac{B_2\lambda^2}{\lambda^2 - C_2} + \frac{B_3\lambda^2}{\lambda^2 - C_3}, \quad (1)$$

with the coefficients presented in Table 2 [ $\lambda$  is given in micrometers in Eq. (1)]. The extinction coefficient of BK7 in the considered wavelength region is zero. Note that we use rounded-off values to simplify data management.

The substrate is semi-infinite; therefore, the reflectance from the backside should not be taken into account. We provide *a priori* information on chemical composition of the coatings. It consists of  $\text{Nb}_2\text{O}_5$  and  $\text{SiO}_2$  materials, but material layer arrangement and layer number within this design are unknown. The refractive indices of  $\text{Nb}_2\text{O}_5$  and  $\text{SiO}_2$  are described by the Cauchy formula

$$n(\lambda) = A_0 + \frac{A_1}{\lambda^2} + \frac{A_2}{\lambda^4}. \quad (2)$$

The coefficients of the Cauchy formula for  $\text{Nb}_2\text{O}_5$  and  $\text{SiO}_2$  are taken from [1] and presented in Table 3 [ $\lambda$  is given in micrometers in Eq. (2)].

To simulate possible refractive index differences, including the presence of contaminants in the production process, we added refractive index offsets and possible absorption to both materials. For each layer, these perturbation factors can be different, thereby simulating some instability of the deposition process. For both layer material refractive indices, we introduce five refractive index wavelength-independent offsets  $\Delta_m$ :

**Table 2. Coefficients of the Substrate Sellmeier Formula Eq. (1)**

$B_1$	$B_2$	$B_3$	$C_1$	$C_2$	$C_3$
1.03961	0.23179	1.01047	0.006	0.02	103.56

**Table 3. Cauchy Formula Coefficients Eq. (2) of  $\text{Nb}_2\text{O}_5$  and  $\text{SiO}_2$  Layer Materials**

Material	$A_0$	$A_1$	$A_2$
$\text{Nb}_2\text{O}_5$	2.218485	0.021827	3.99968e-3
$\text{SiO}_2$	1.460472	0.0	4.9867e-4

**Table 4. Extinction Coefficients of Formula Eq. (4) of Nb<sub>2</sub>O<sub>5</sub> Layer Material**

Absorption	Index <i>j</i>	<i>D</i> <sub>1</sub>	<i>D</i> <sub>2</sub>	<i>D</i> <sub>3</sub>
“Weak”	1	4.0e + 5	56.0	1.0e-10
“Standard”	2	3.0e + 5	50.0	1.0e-8
“Strong”	3	4.0e + 4	40.0	1.0e-6

$$n_m(\lambda) = n(\lambda) + \Delta_m, \Delta_m = 0.005(m - 3), m = 1, \dots, 5. \tag{3}$$

The extinction coefficient is described by the equation ( $\lambda$  is given in micrometers)

$$k(\lambda) = D_1 \exp(-D_2\lambda) + D_3. \tag{4}$$

Equation (4) has typical wavelength dependency, providing higher absorptance at shorter wavelengths. Only Nb<sub>2</sub>O<sub>5</sub> has absorptance; all coefficients in Eq. (4) for SiO<sub>2</sub> are zeros. Possible values of Eq. (4) for Nb<sub>2</sub>O<sub>5</sub> are presented in Table 4, corresponding to “weak,” “standard,” and “strong” absorptance. The last case can be associated with possible unknown contaminants during the production process.

Therefore, the complex refractive index is

$$\tilde{n}(\lambda) = n(\lambda) + \Delta_m - ik_j(\lambda), \tag{5}$$

where  $n(\lambda)$  is given by Eq. (2),  $\Delta_m$  is the variation of the real refractive index Eq. (3), and  $k_j(\lambda)$  is zero for SiO<sub>2</sub> and given by formula Eq. (4) for Nb<sub>2</sub>O<sub>5</sub> with coefficients selected from Table 4 according to a value of the index  $j$ . Figure 1 shows possible refractive index and extinction coefficients for Nb<sub>2</sub>O<sub>5</sub>; in total, it provides 15 possible combinations for the complex refractive index of Nb<sub>2</sub>O<sub>5</sub>. On the other hand, there are only five different refractive index variants for SiO<sub>2</sub> layer material. All these variations of Nb<sub>2</sub>O<sub>5</sub> and SiO<sub>2</sub> can be present in the black box designs.

Note that variations of the refractive indices in the black box designs are not completely random. We tried to provide some correlations between adjacent layers of the same material, not allowing too abrupt changes of the refractive index and extinction coefficient. In general, it corresponds to slowly varying instability factors during a deposition process.

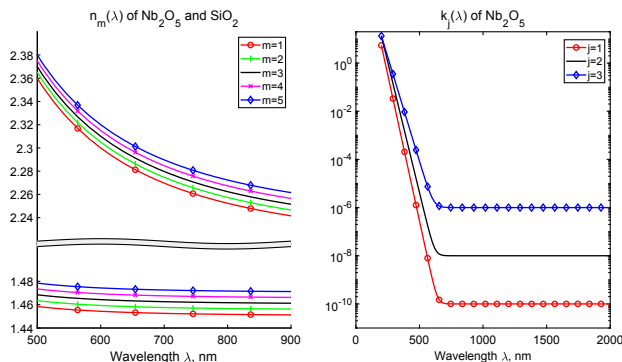


**Fig. 1.** Possible refractive index and extinction coefficient wavelength dependencies for Nb<sub>2</sub>O<sub>5</sub> and SiO<sub>2</sub> layer materials.

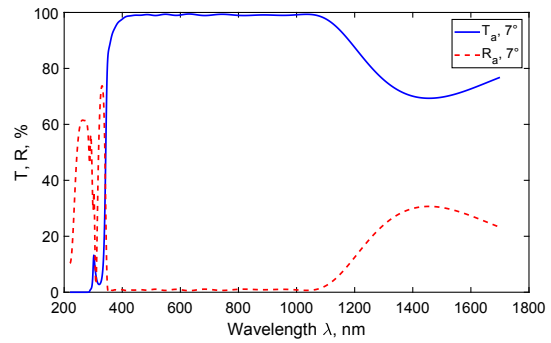


**Fig. 2.** Reflectance and transmittance of the antireflection coating at 7°, see Data File 1 for underlying values [2].

**B. Problem A.1: Black Box Antireflection Coating**

The “measurement” data  $\hat{R}_a(\lambda)$  (reflectance of averaged polarization) and  $\hat{T}_a(\lambda)$  (transmittance of averaged polarization) at 7° incidence (Fig. 2) are available as Data File 1 [2].

This is a three-column comma-separated values file with the wavelength in nanometers in the first column,  $\hat{T}_a(\lambda)$  in the second, and  $\hat{R}_a(\lambda)$  in the third. The wavelength changes in the range of 220–1700 nm with steps of 1 nm. The first line is the header line indicating the data in columns, and the rest of the lines contain the data.

We estimate the submissions using the merit function (MF)  $D_1$ :

$$D_1 = \left\{ \frac{1}{2 \cdot 1481} \sum_{\lambda=220}^{1700} [R_a(\lambda) - \hat{R}_a(\lambda)]^2 + [T_a(\lambda) - \hat{T}_a(\lambda)]^2 \right\}^{1/2}. \tag{6}$$

Here,  $\hat{T}_a(\lambda)$  and  $\hat{R}_a(\lambda)$  are the “measurement” data, and  $T_a(\lambda)$  and  $R_a(\lambda)$  are transmittances and reflectances of the non-polarized light of the submitted solution, respectively.

The physical thickness of the AR coating cannot be greater than 3500 nm, and the number of layers cannot exceed 35. Solutions violating these limits are not accepted. The winner is defined on the basis of the MF Eq. (6).

The AR black box design has 22 layers with the layer material distribution shown in Fig. 3. More abrupt changes of material properties (compare high index layers 1 and 3, low index layers 2 and 4) simulate typical instabilities at the beginning of the deposition process. Note also that we provided transmittance and reflectance data in the UV range of 220–370 nm, where quite informative spectral features are located. Since the absorptance of different Nb<sub>2</sub>O<sub>5</sub> variants is also quite different in the UV range, it improves the chances to solve the AR black box problem.

**C. Problem A.2: Short-Wavelength Pass, Non-Polarizing Filter**

A SWPNPF was designed for 45° incidence (Fig. 4) with the separation wavelength of 900 nm. For this problem, a virtual, web-based spectrophotometer should be used to obtain

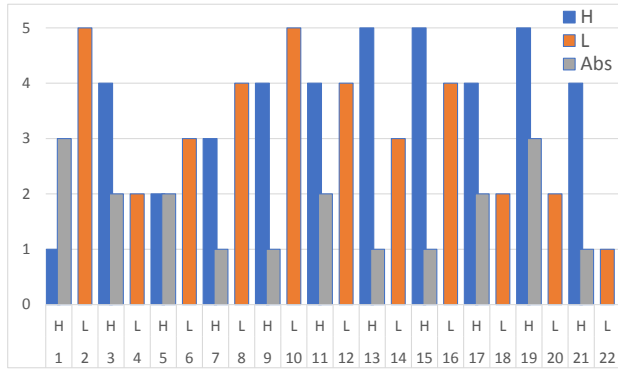


**Fig. 3.** Distribution of materials in AR black box design (see Data File 2, Ref. [8] for underlying values and layer thicknesses).

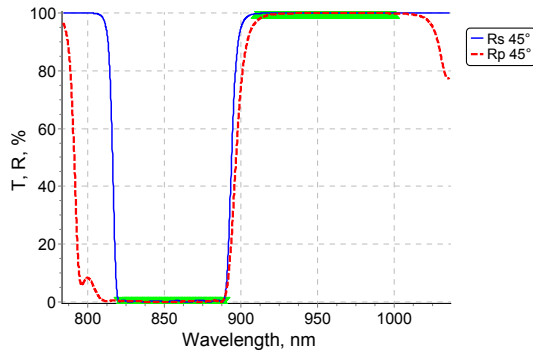


**Fig. 4.** Reflectance of the short-wave pass filter at 45° for  $s$ - (blue solid) and  $p$ -polarized (red dashed) light. Target specifications for the reflectance are shown with thick, solid green horizontal lines.

“measurement” spectra for different angles of incidence and polarizations. Minimum allowed wavelength step is 0.1 nm (configurable). Wavelength limits can be selected in the range of 220–1700 nm. Angle of incidence can be from 0° (normal incidence) up to 65° for transmittance and from 7° to 60° for reflectance. It is possible to obtain  $s$ -,  $p$ -, and average-polarized spectral characteristics for each of the angles of incidence. Note that the virtual spectrophotometer provides accurate values of spectral characteristics without any measurement errors.

We estimate the submissions using the MF  $D_2$ :

$$D_2 = \left\{ \frac{1}{6 \cdot 1481} \sum_{\lambda=220}^{1700} \left( \left[ R_a(\lambda, 7^\circ) - \hat{R}_a(\lambda, 7^\circ) \right]^2 + \left[ T_s(\lambda, 7^\circ) - \hat{T}_s(\lambda, 7^\circ) \right]^2 + \left[ R_s(\lambda, 60^\circ) - \hat{R}_s(\lambda, 60^\circ) \right]^2 + \left[ T_p(\lambda, 60^\circ) - \hat{T}_p(\lambda, 60^\circ) \right]^2 + \left[ R_p(\lambda, 60^\circ) - \hat{R}_p(\lambda, 60^\circ) \right]^2 + \left[ T_r(\lambda, 60^\circ) - \hat{T}_r(\lambda, 60^\circ) \right]^2 \right) \right\}^{1/2}. \quad (7)$$

Reflectance  $\hat{R}_{s,p}$  and transmittance  $\hat{T}_{s,p}$  “measurements” of the black box SWPNPF at 7° and 60° can be found in Data

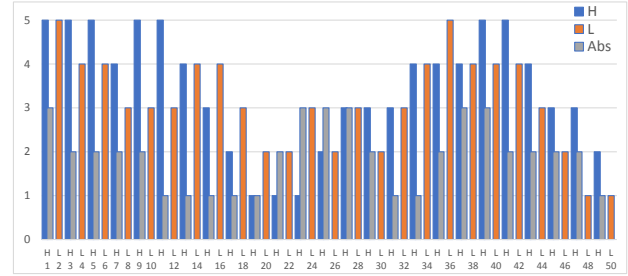


**Fig. 5.** Distribution of materials in SWPNPF black box design (see Data File 4, Ref. [9] for underlying values and layer thicknesses).

File 3 [3]; it allows to evaluate  $D_2$  without access to a virtual spectrophotometer.

It is additionally known that the short-wavelength pass filter cannot be thicker than 12  $\mu\text{m}$  total physical thickness, and the number of layers cannot exceed 75. Solutions violating these limits are not accepted. The winner is defined on the basis of the MF Eq. (7).

The SWPNPF black box design has 50 layers with the layer material distribution shown in Fig. 5. We arranged the distribution of materials without abrupt changes between layers of the same material. Since the transmittance is high for shorter wavelengths, it improves chances to solve the black box problem, since simulated measurements are quite informative in the range of different absorptances of  $\text{Nb}_2\text{O}_5$ .

## D. Problem A – Evaluation of the Results

According to the design contest, the evaluation criteria are MFs  $D_1$  Eq. (6) and  $D_2$  Eq. (7). To present better how close are refractive index profiles of submitted solutions to the black box coating, we also introduce additional metrics for the refractive index and extinction coefficient:

$$\Delta_n = \frac{1}{D} \int_0^D |n(x) - n_{\text{bbox}}(x)| dx, \quad (8)$$

$$\Delta_k = \frac{1}{D} \int_0^D |k(x) - k_{\text{bbox}}(x)| dx, \quad (9)$$

where  $x$  is the coordinate along coating cross section, “bbox” designates the refractive index and extinction coefficient profiles of the black box design, and  $D$  is the maximum physical thickness of coatings under comparison. The profile of a thinner coating is extended with the refractive index of air (equal to 1.0); therefore, any difference between physical thicknesses strongly contributes to these metrics.

Note that these additional evaluation metrics are not possible to use in the contest because one can easily organize a procedure of the solution search based on direct optimization of the criteria Eqs. (8) and (9) received from the evaluation software server in an optimization loop, thus completely avoiding any optics-related computations. These metrics are presented among with the evaluation criteria in Supplement 1.

## E. Problem A.1 Contest Results

The 18 submissions (including three late submissions) to the AR Coating Black Box Challenge were evaluated, and the results

**Table 5. Black Box AR Challenge Results Summary<sup>a</sup>**

Designer	Place	#	$N$	$D_1$	$\Delta_n$	$\Delta_k$
Lemarchand	1	1	22	0.000 E + 00	0.0000	0.0000
Southwell and Peeples	2	2	35	7.692 E-06	0.0166	0.0130
Yuan	3	3	35	1.348 E-05	0.0562	0.0657
Yuan	4	4	35	1.436 E-05	0.0587	0.0678
Tonova	5	35	35	1.635 E-05	0.0366	0.0307
	** <sup>c</sup>	6	23	8.171 E-05	0.0356	0.0284
	** <sup>c</sup>	7	22	9.907 E-05	0.0369	0.0314
		8	35	9.999 E-05	0.0589	0.0685
		9	34	1.342 E-03	0.0815	0.1088
		10	34	1.556 E-03	0.1303	0.1459
		11	35	1.676 E-03	0.3275	0.4096
		12	35	4.381 E-03	0.2172	0.2605
		13	33	4.564 E-03	0.2193	0.2413
		14	35	8.166 E-03	0.3475	0.4904
		15	35	8.771 E-03	0.3440	0.4234
		16	30	9.759 E-03	0.1812	0.2635
		17	35	1.659 E-02	0.3160	0.4193
	* <sup>b</sup>	18	35	3.406 E-02	0.0177	0.1919

<sup>a</sup># is the design number in Fig. 6,  $N$  is the number of design layers,  $D_1$  is presented by Eq. (6), and  $\Delta_n$  and  $\Delta_k$  are additional criteria of profile closeness Eqs. (8) and (9).

<sup>b</sup>\* Late submissions.

<sup>c</sup>\*\* Late submissions after design contest presentation.

are summarized in Table 5. All submissions fulfilled formal requirements for the limit of layer number and total physical thickness. Some submissions did not follow file formatting rules (e.g., using a wrong decimal separator), which means that the designers did not use online evaluation software to check the results before submission. Such files were adjusted manually during evaluation to conform to the contest specifications. We also included three late submissions marked with asterisks in Table 5.

The refractive index profiles of all 18 submissions at wavelength 600 nm are shown in Fig. 6. The numbers in Fig. 6 corresponds to the column # in Table 5. In Supplement 1, one can also find extinction coefficient profiles at wavelength 250 nm and discrepancies of non-polarized light reflectance and transmittance at a 7° angle of incidence.

Lemarchand was the winner of the AR Black Box Contest; he was able to find the solution exactly matching the black box 22-layer AR design. All three metrics  $D_1$ ,  $\Delta_n$ , and  $\Delta_k$  are 0.0. Second and third places were won by Southwell and Peeples, and Wenjia Yuan, correspondingly. These submissions are designs with maximum allowed number of layers with an attempt to reach as low a  $D_1$  value as possible. Design #5 by Tonova with a somewhat higher value of  $D_1$  demonstrates an important fact: low values of the discrepancy do not always correspond to solutions close to the “ground truth” (black box design in our case). Indeed, design #5 provides values of  $\Delta_n$ ,  $\Delta_k$  less than designs #3 and #4. Very late submissions marked by \*\* in Table 5 were submitted after the presentation of contest results; therefore, the number of layers in AR black box design became known to this designer. These post-deadline solutions provide rather good values of evaluation metrics, and this is an illustration of

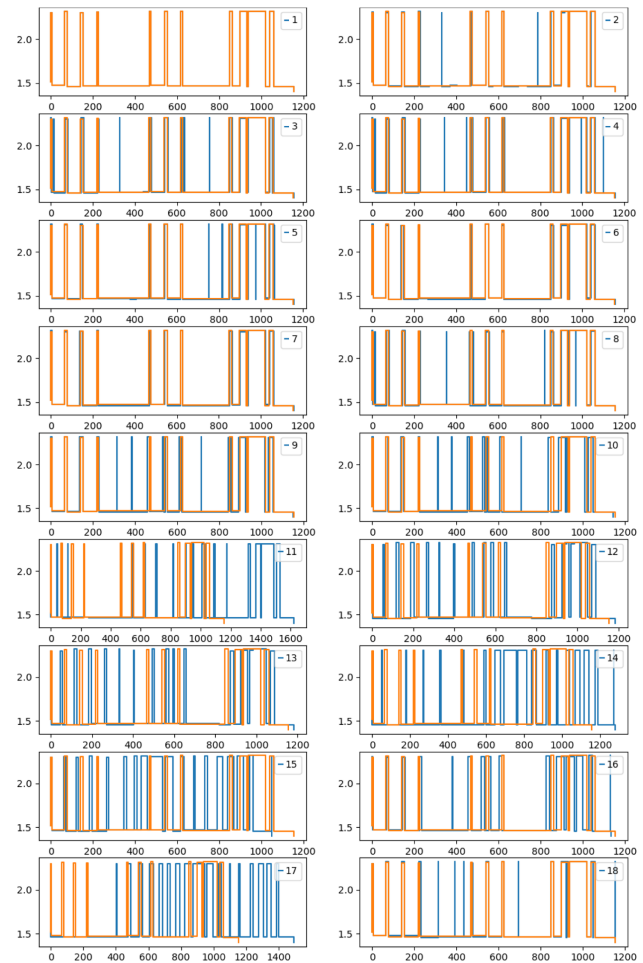


**Fig. 6.** Refractive index profiles of the submitted designs at 600 nm; orange line is the black box AR, and blue lines are submissions. Designs 6, 7, and 18 are late submissions.

importance of the so-called *a priori* information in the reverse-engineering process. In this case, the expected number of design layers plays the role of this additional information.

**F. Problem A.2 Contest Results**

The 12 submissions to the SWPNPF Coating Black Box Challenge were evaluated (including one late submission), and the results are summarized in Table 6.

The refractive index profiles of all 12 submissions at wavelength 600 nm are shown in Fig. 7. The numbers in Fig. 7 correspond to the column # in Table 6. In Supplement 1, one can also find extinction coefficient profiles at wavelength 250 nm and discrepancies of non-polarized light reflectance and transmittance at a 7° angle of incidence.

Lemarchand won the SWPNPF Black Box Contest with the first prize; he was able to find the solution exactly matching the black box 50-layer SWPNPF design. All three metrics  $D_1$ ,  $\Delta_n$ , and  $\Delta_k$  are 0.0. Second and third places were won by Southwell and Peeples, and Tonova, correspondingly. It is worthwhile to note that designs #2–#5 use almost the maximum allowed by contest rules number of layers (75 in this case) to minimize the evaluation criterion  $D_2$  as much as possible. Another note is

**Table 6. Black Box SWPNPF Challenge Results Summary<sup>a</sup>**

Designer	Place	#	$N$	$D_2$	$\Delta_n$	$\Delta_k$
Lemarchand	1	1	50	0.000 E + 00	0.0000	0.0000
Southwell and Peeples	2	2	75	5.339 E-04	0.4285	0.5905
Southwell and Peeples	3	3	75	5.362 E-04	0.4285	0.5894
Tonova	3	4	75	1.762 E-03	0.0130	0.0228
Tonova		5	74	2.096 E-03	0.0095	0.1001
		6	64	3.551 E-02	0.1548	0.3083
		7	75	3.793 E-02	0.1667	0.3239
	<sup>b</sup> *	8	75	7.787 E-02	0.4254	0.7282
		9	74	1.195 E-01	0.4522	0.5248
		10	39	1.453 E-01	0.4843	0.6536
		11	52	2.553 E-01	0.4654	0.6072
		12	73	2.779 E-01	0.2855	0.6451

<sup>a</sup># is the design number in Fig. 7,  $N$  is the number of design layers,  $D_2$  is presented by Eq. (7), and  $\Delta_n$  and  $\Delta_k$  are additional criteria of profile closeness Eqs. (8) and (9).

<sup>b</sup>\* Late submission.

again related to the values of  $D_2$  compared to additional criteria  $\Delta_n$ ,  $\Delta_k$ . Designs #4 and #5 by Tonova (third place) provide much lower values of  $\Delta_n$ ,  $\Delta_k$  compared to designs #2 and #3 by Southwell and Peeples (second place), in spite of the higher values of the main evaluation criterion  $D_2$ .

### G. Problem A – Design methods

Both Problems A.1 and A.2 had a very high risk of the necessity to apply a tie breaker rule, since potentially several designers could obtain exactly the same black box solution. The tie breaker rule was the quality of the design approach description (informative, carefully written, detailed, etc.). Since only Lemarchand was able to find black box solutions (and he also provided a very detailed description, briefly summarized below), this rule was not required; nevertheless, the designers were motivated to describe their design methods.

Lemarchand mentioned that he used a very similar approach to the both Problems A.1 and A.2. He used OptiLayer Thin Film software for computations on a mid-range laptop computer. First, he selected two materials, H32 and L3, with an average index and searched for an “acceptable” solution using a random search approach. He used design contest limits for the number of layers: 35 for Problem A.1 and 75 for Problem A.2. He used the whole target for Problem A.1 and virtual “measurements” in the range of 400–1700 nm for Problem A.2. After approximately 12 h of random search, he was able to estimate roughly the number of layers in the black box designs (about 25 and about 60, respectively).

As the second iteration, Lemarchand used a random search procedure again, but in this case around roughly estimated designs from the first iteration. In addition, he removed several very thin layers and finally was able to find expected numbers of layers (22 and 50, respectively). He made an additional check: removing any layer from these designs leads to a dramatically strong increase in the MF.

Probably the most time-consuming step was turning a design consisting of the two materials H32 and L3 into a solution with

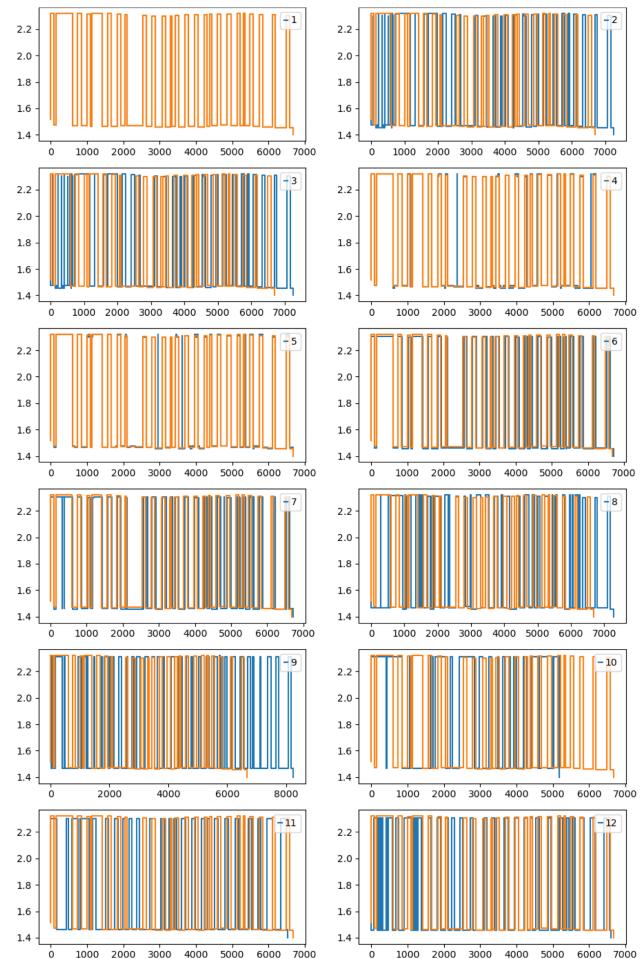


**Fig. 7.** Refractive index profiles of the submitted designs at 600 nm, orange line is the black box AR, and blue lines are submissions. Design 8 is a late submission.

a full range of material selections. In this case, he used the full spectral range available in a virtual spectrophotometer and two angles of incidence: 7° (non-polarized) and 60° (both  $s$  and  $p$  polarizations). Lemarchand applied multiple *Deep Needle Search* procedures accompanied by a subsequent *Design Cleaner*. In addition, he applied manual adjustments of the designs, merging some indices to intermediate values. These steps, repeated many times (50–100), allowed to decrease the MF even further, keeping the number of layers slightly higher than previously estimated values. Finally, this process allowed to obtain the final result for Problem A.2 and a design with  $D_1$  of about 1.0e-4 for Problem A.1.

Lemarchand also mentioned that the AR black box problem required additional work on the design, since for layers of thickness in the range of 5–15 nm, the sensitivity of  $D_1$  to small variations of the refractive index is rather low. Using sensitivity analysis, Lemarchand excluded sensitive layers from further considerations and further divided non-sensitive layers into sublayers, for example: H33 layer of thickness  $d$  can be divided into three sublayers H23/H33/H43 of thickness  $d/3$ . In total, approximately 10 layers were subjected to this operation. After an additional random search around this design and additional

manual cleanup steps, he was able to obtain the black box solution of AR Problem A.1 as well.

Southwell and Peeples provided a brief description of their approach. They applied a Flip-Flop approach to evaluate the MFs. Each layer was cycled through all 15 materials to see which one lowers the MF. The method worked well given a fixed number of layers. For a high number of layers, this procedure provided very good fits. They did not investigate lower numbers of layers due to lack of time.

Tonova used numerical design algorithms available in the software OptiLayer for both problems. For the AR problem, she first found a good starting design using reflection and transmission data only in the spectral region with low reflection and the spectral region where the material absorption is low (350–1700 nm) with only two layer materials: H32 and L1. Tonova found a starting design consisting of 28 layers with total thickness 1162 nm with a good fit of the spectral data. After that, she repeated the needle optimization technique and subsequent design cleaning procedures multiple times to insert new layers in the design and to fit the data in the whole spectral region of 220–1700 nm. At this time, more possible layer materials have been allowed, restricted to L1, L3, L5, H11, H1, H13, H31, H32, H33, H51, H52, and H53.

For SWPNPF Problem A.2, Tonova again started with only two materials, and with three quarter-wave stacks that reproduce approximately the width and position of the reflection maxima of  $p$  and  $s$  polarizations at a  $60^\circ$  angle of incidence. After refining this start design using also the reflection of  $p$  and  $s$  polarizations at an angle of incidence of  $45^\circ$  as well as the reflection at an angle of incidence of  $7^\circ$ , she was able to find a design that fits relatively well the reflection data. This design has a total thickness was 6734 nm and consists of 51 layers and fits also relatively well the whole spectral region from 220 to 1700 nm. This design was also subjected to multiple needle optimization steps and subsequent design cleaning procedures with the same subset of allowed materials: L1, L3, L5, H11, H1, H13, H31, H32, H33, H51, H52, and H53.

Ruiz provided a description of his approach to AR Problem A.1. He used GPU-based computations, optimization randomized with respect to material selection designs with a Levenberg–Marquardt method, and then applying a needle-optimization step to an improved design, followed by CPU-based Levenberg–Marquardt optimization.

Bolshakov briefly commented that he used FilmStar software and some custom code. He fitted in the visible range, trying to determine the number of layers, then applied random changes of refractive indices. He provided solutions to the AR black box problem only.

Perilloux submitted the first design created of two materials only, and his second design created from this two-material design by insertions of available coating materials. He mentioned that several optimization methods were used together with adjustments of weighting factors with emphasis on replicating the three spectral spikes in the UV wavelength region without further details.

Other participants did not provide details on their approach to the Black Box Challenge.

### 3. PROBLEM B: MULTI-BANDPASS FILTERS FOR 3D CINEMA PROJECTION

Problem B involves creating two white-balancing, multi-spectral filters for a set of 3D cinema glasses that will be used by your extended family for an outdoor theater. Your projector has been optically modified to create two sets of offset images to create the necessary parallax. You need an additional effect through either polarization or color metamerism to complete the 3D experience. Due to the pandemic, polarizers are in short supply. Fortunately, you have a coating facility and eyewear frames with lenses that you can coat. You also have enough glass to replicate each filter to be placed in the projector such that the projector channels can be color-matched for the appropriate eye as illustrated in Fig. 8.

The goal of this challenge was to create multilayer coating designs for left and right filters that will be placed in the projector and in the eye frames to meet the specification at  $20^\circ\text{C}$ , and limit the transmission change for cold and hot outdoor temperatures. Each material will have a specific change of refractive index with temperature ( $dn/dT$ ) (Table 7). The projector will stay at the specified  $20^\circ\text{C}$ , but the glasses will experience a temperature change based on the outdoor temperature.

The projector has the appropriate optics to divide the image into two separate paths to be offset on the projection screen. However, the projector has only one set of red, green, and blue LEDs inside. The LED RGB spectrum is shown in Fig. 9. To fully create the 3D effect, the designer will need to split the wavelength regions for each LED such that only half of each spectrum (R, G, and B) will end up in each eye, therefore enabling the color metamerism effect. The wavelength spectra may be split as indicated in Table 8.

For example, if Spectrum 1 is included for the blue (B) in the left eye, Spectrum 2 will represent B in the right eye. Spectrum 1 and Spectrum 2 have high transmission regions that are in opposite spectral bands. Both spectra will divide each color LED in half for all three color channels (R, G, and B). Cross talk between the left and right eyes is minimized. A transmission example where both surfaces of the left and right eye lenses are coated is shown in Fig. 10. The left eye filter in the example transmits B1, G1, and R1, and the right eye filter transmits B2, G2, and R2.

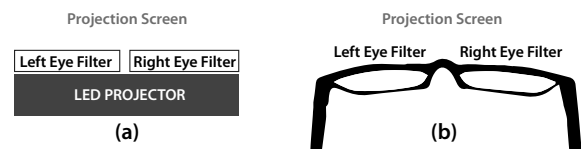


Fig. 8. Positions of left and right eye filters: (a) in projector and (b) in cinema glasses.

Table 7. Index of Refraction for the Substrate, Medium, and Each Material at  $-50^\circ$ ,  $20^\circ$ , and  $+50^\circ$

$^\circ\text{C}$	Substrate	H	L	F	T	M
$-50^\circ\text{C}$	1.513	2.131	1.499	1.811	2.101	1.359
$+20^\circ\text{C}$	1.52	2.250	1.450	2.000	2.150	1.380
$+50^\circ\text{C}$	1.523	2.301	1.429	2.081	2.171	1.389

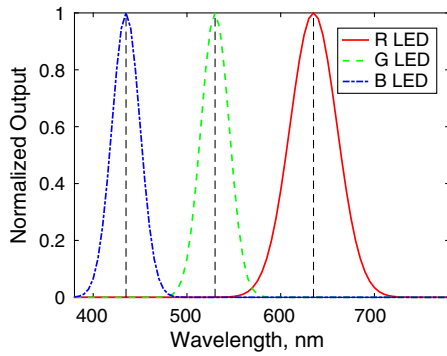


Fig. 9. RGB light source.

**Table 8. Wavelength Bands (Spectrum 1 or Spectrum 2) for Each Color Primary without LED Source (i.e., with Uniform Spectral Illumination)<sup>a</sup>**

Color	Spectrum 1	
LED	30% > T ≥ 100%	T < 1%
Blue (B)	380–435 nm	440–474 nm
Green (G)	480–530 nm	539–568 nm
Red (R)	580–635 nm	642–780 nm
Color	Spectrum 2	
LED	T < 1%	30% > T ≥ 100%
Blue (B)	380–432 nm	436–480 nm
Green (G)	485–525 nm	531–570 nm
Red (R)	586–626 nm	636–780 nm

<sup>a</sup>Spectrum 1 and Spectrum 2 are evaluated every 0.1 nm.

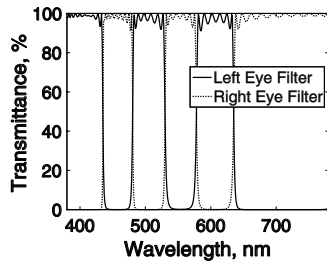
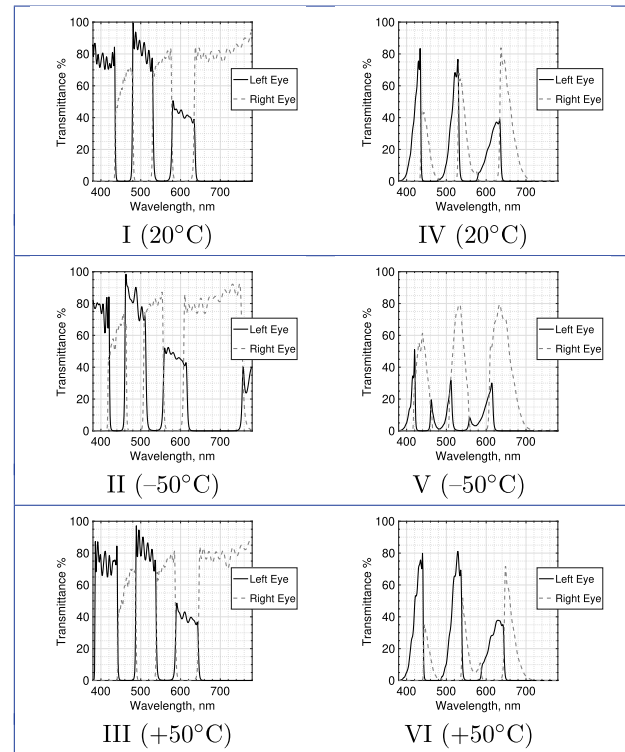


Fig. 10. Example of bandpass filters for left and right eyes.

These filters also need to be white-balanced so that all of the images produced by the projector will appear to be the same color. Each filter has two surfaces that can be coated; as such, the total transmission can be maximized and white-balanced. The process to determine the color of the filters is to calculate the tristimulus values (XYZ) from the transmittance of the left or right filter, using the 10° observer color-matching functions and the projector's LED source from 380–780 nm, every 1 nm (data from Program of Color Science, at Rochester Institute of Technology [[4]]). When CIELAB values are calculated using the filter's XYZ tristimulus values, the white points (XYZ<sub>w</sub>) used for comparison will be those calculated from daylight (D65) and the 10° color-matching functions for the formulas in Eqs. (14) and (11).

The example filter shown in Fig. 11. I transmits B1, G1, and R1 for the left eye using three bandpass filters on the front surface and the color-correcting coating on the back. The right



**Fig. 11.** (I) Wavelength distribution for two example filters at 20°C: left eye high %T is B1, G1, and R1 (solid). Right eye high %T is B2, G2, and R2 (dashed), which meet specifications in Table 8. Both filters are at normal incidence with coated front and back surfaces of the substrate without LED light source. (IV) Filters in I transmitting the LED light source through the left and right eye filters. (II) Same filter transmission as I, but at -50°C, (V) filters with LED spectrum at -50°C; (III) same filter transmission as I, but at +50°C, (VI) filters with LED spectrum at +50°C.

eye filter transmits B2, G2, and R2 where the front surface is also a multiple bandpass filter and the back surface is the color-correcting coating. The design example shown in Fig. 11.II has both filters using the LED source, to produce a white point in CIELAB for D65 and 10° observer from 380–780 nm, every 1 nm:

$$\begin{aligned} X_n &= 94.8107, \\ Y_n &= 100.0000, \\ Z_n &= 107.3040, \end{aligned} \quad (10)$$

$$L^* = 116 f(Y/Y_n) - 16,$$

$$a^* = 500 [f(X/X_n) - f(Y/Y_n)],$$

$$b^* = 200 [f(Y/Y_n) - f(Z/Z_n)],$$

$$f(x) = \begin{cases} (x)^{1/3}, & x > 0.008856 \\ 7.787x + 16/116, & x \leq 0.008856 \end{cases} \quad (11)$$

The submitted designs will be based on the refractive index materials found in Table 7 for 20°C, which will be the temperature that will be maintained in the projector. The color transmitted using the projector's LED spectrum for each of the

two filters at 20°C will measure CIELAB color coordinates in  $a^*$  and  $a^*$  coordinates at  $0.0 \pm 0.4$  and  $0.0 \pm 0.4$ , respectively (D65, 10° observer). The designs' transmitted spectra are converted to CIELAB color coordinates so that the amount of light transmitted through these filters can be calculated by using the CIELAB value for lightness, or  $L^*$ .

Submitted designs for the left and right filters were accepted that met the following criteria at 20°C.

1. The angle of incidence for both left and right eye coatings will be 0° (i.e., normal incidence).
2. Meet the Spectrum 1 and Spectrum 2 transmittance requirements in Table 8 for the filters without using the LED projector source (i.e., using uniform spectral illumination across the visible wavelength region). Spectrum 1 and Spectrum 2 transmittance requirements in Table 8 will be evaluated every 0.1 nm across 380–780 nm.
3. Using the LED source to obtain a white point that is similar to a D65 reference white, use the 10° observer color-matching functions from 380–780 nm every 1.0 nm to obtain CIELAB  $a^*$  and  $b^*$  coordinates equal  $0.0 \pm 0.4$  and  $0.0 \pm 0.4$ , respectively.
4. Each filter should receive one of the red, green, and blue LED spectra from R1, R2, G1, G2, B1, and B2 (see Table 8).
5. The CIELAB transmitted lightness,  $L^*$ , using the projector's LED spectrum for either filter (both surfaces) will be  $\geq 60$ .
6. Designs submitted will use only +20°C index data for the layer materials from Table 7.
7. No layer thickness for any surface design will be  $< 5$  nm.
8. No single surface design can exceed 100 layers total.
9. Each surface of the two filters will be coated with at least one layer.

The designer indicated whether the design should be used for cold temperature, hot temperature, or both in the design submission. Each designer could submit up to two pairs of designs per cold temperature and two pairs for hot temperature (designs for the right and left eyes are considered one pair, four coated surfaces). If the designs are to be used for both temperatures, then a total limit of four submissions will be permitted.

The designs in Figs. 11.I and IV, are the white-balanced transmittance for both left and right eyes at 20°C. When the designs are used at a very cold or very hot temperature, the physical thicknesses of all of the layers will stay the same, but the design will shift based on the refractive indices of materials at different outdoor temperatures. The refractive indices for all layer materials for  $-50^\circ\text{C}$  and  $+50^\circ\text{C}$  (worst case) are given in Table 7. The transmitted color changes for the design example for  $-50^\circ\text{C}$  are shown in Figs. 11.II and V, and  $+50^\circ\text{C}$  in III and VI. The designer must calculate the outdoor MF,  $\text{MF}_O$  [Eq. (14)]. The  $\text{MF}_O$  is broken down into three main parts.

1. The first part adds the color differences ( $\Delta E$ ) of the left and right filters between the projector (P) temperature [20°C] and the outdoor temperature (O), with an appropriate weighting [see Eqs. (12)–(14)].
2. The second part calculates the absolute value of the deviation between the left eye filter and right eye filter color

difference between the projector and the outdoor temperature. The closer the two color differences ( $\Delta E$ ) for the left and right lenses, the smaller this part of the equation. It is important not only to have a small color shift, but also it should be relatively equal for both left and right filters.

3. The last part is based on the  $L^*$  value for both filters at 20°C (in the projector, P). The higher  $L^*$  is for the initial submitted design at 20°C, the lower that value will become.

The winning design minimized the color change due to the outdoor temperature, while maximizing the amount of transmitted light,  $L^*$ , at 20°C. The  $\text{MF}_O$  was calculated for the example design; a value of 11.053635 was calculated for  $-50^\circ\text{C}$  and 5.806175 for  $+50^\circ\text{C}$ :

$$\begin{aligned} \Delta L_{\text{left},O}^* &= L_{\text{left},P}^* - L_{\text{left},O}^*, \\ \Delta a_{\text{left},O}^* &= a_{\text{left},P}^* - a_{\text{left},O}^*, \\ \Delta b_{\text{left},O}^* &= b_{\text{left},P}^* - b_{\text{left},O}^*, \end{aligned} \tag{12}$$

$$\begin{aligned} \Delta L_{\text{right},O}^* &= L_{\text{right},P}^* - L_{\text{right},O}^*, \\ \Delta a_{\text{right},O}^* &= a_{\text{right},P}^* - a_{\text{right},O}^*, \\ \Delta b_{\text{right},O}^* &= b_{\text{right},P}^* - b_{\text{right},O}^*, \end{aligned} \tag{13}$$

$$\begin{aligned} \Delta E_{\text{left},O} &= \sqrt{(\Delta L_{\text{left},O}^*)^2 + (\Delta a_{\text{left},O}^*)^2 + (\Delta b_{\text{left},O}^*)^2}, \\ \Delta E_{\text{right},O} &= \sqrt{(\Delta L_{\text{right},O}^*)^2 + (\Delta a_{\text{right},O}^*)^2 + (\Delta b_{\text{right},O}^*)^2}, \end{aligned} \tag{14}$$

$$\begin{aligned} \text{MF}_O &= \left( \frac{\Delta E_{\text{left},O}}{20} + \frac{\Delta E_{\text{right},O}}{20} \right) + |\Delta E_{\text{left},O} - \Delta E_{\text{right},O}| \\ &+ \left( (70/L_{\text{left},P}^*) + (70/L_{\text{right,max},P}^*) \right). \end{aligned} \tag{15}$$

### A. Problem B – Design Submissions

Designer Javier Ruiz was the only designer to submit designs for Problem B (see Table 1). He submitted four designs to be used for both outdoor temperatures, and he accompanied his designs with the strategy used to solve the problem [5]. Since the designer did not have any idea what the final temperatures would be, each design was optimized for a different temperature region:

- design 1  $\rightarrow +30^\circ\text{C}$  to  $+50^\circ\text{C}$ ;
- design 2  $\rightarrow -50^\circ\text{C}$  to  $-40^\circ\text{C}$ ;
- design 3  $\rightarrow -35^\circ\text{C}$  to  $-15^\circ\text{C}$ ;
- design 4  $\rightarrow -10^\circ\text{C}$  to  $+10^\circ\text{C}$ .

In the correspondence [5], Ruiz commented: *Custom software was written to tackle this design challenge. Parallelization was implemented using NVIDIA GPU. The GPU code was written in CUDA. The interface code to the GPU CUDA code was written in c++. The GUI and c++ interface code was written in C#. Using the starting design provided by the contest,*

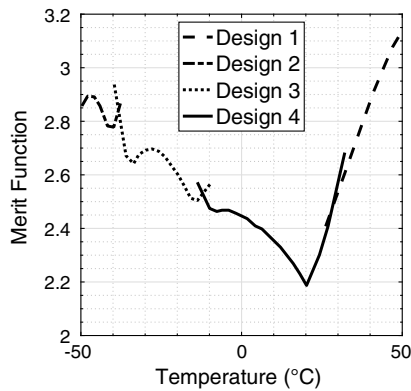


**Fig. 12.** Problem B: merit function of four submitted designs versus temperature in °C.

**Table 9.** Ranking of Ruiz Designs for Inuvik, Canada, by Merit Function

Design	Place	MF
4	1	2.459131
2	2	2.634037
1	3	3.163727
3	4	3.942649

both left and right designs were optimized for minimum  $\Delta E$  over temperature. As both left and right designs were optimized, each improvement of the design was recorded for subsequent matching.

Ruiz’s designs are plotted in Fig. 12 by temperature range versus MF.

On 11 May 2022, the outdoor locations were chosen and their current temperatures were recorded. Inuvik, Canada, was chosen for the cold temperature ( $-3^{\circ}\text{C}$ ), and Kuwait City was chosen for the hot temperature ( $+26^{\circ}\text{C}$ ).

**B. Temperature in Inuvik, Canada ( $-3^{\circ}\text{C}$ )**

The performance of designs 1 through 4 for  $-3^{\circ}\text{C}$  are shown in Fig. 13, and the placement and MFs of all four designs are shown in Table 9. The left column in Fig. 13 shows the transmission shift between the temperature of the filters in the projector and those of the eyewear. The right column shows the transmission difference between the two. One can see that design 1 is very ordered, with very little ripple, where designs 2 through 4 have an incredible amount of ripple in both the transmission bands and the difference plots. Design 4 was the first place design with an MF of 2.459131, as was expected in Fig. 12.

**C. Temperature in Kuwait City, Kuwait ( $+26^{\circ}\text{C}$ )**

The performance of designs 1 through 4 for  $+26^{\circ}\text{C}$  are shown in Fig. 14, and the placement and MFs of all four designs are shown in Table 10. As with Fig. 13, the left column in Fig. 14 shows the transmission shift between the temperature of the filters in the projector and those of the eyewear, and the right shows the transmission difference. The same ripple in the transmission bands does not seem to translate into the extreme ripple difference as with the cold temperature. Design 4 was also the

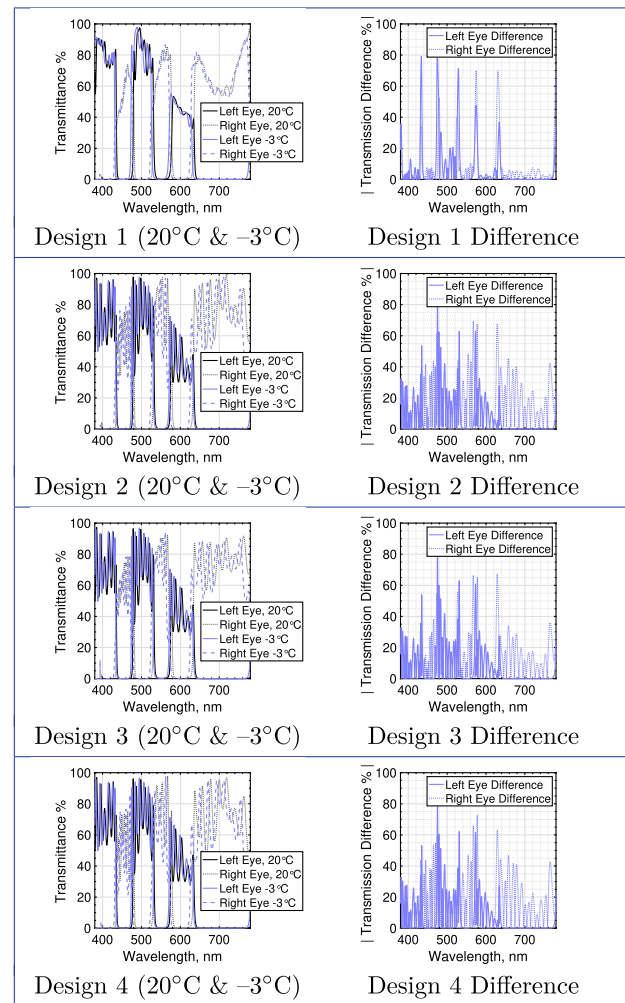


**Fig. 13.** Design comparison for  $20^{\circ}\text{C}$  and  $-3^{\circ}\text{C}$  for designs 1–4. Left column compares projector and outdoor filter performance, and right column compares the differences in performance.

**Table 10.** Ranking of Ruiz Designs for Kuwait City, Kuwait, by Merit Function

Design	Place	MF
4	1	2.367159
1	2	2.399027
2	3	2.482192
3	4	2.896291

first place design with an MF of 2.367159, which is hard to discern in Fig. 12 because of the overlap with design 1.

What the designs show is that significant passband ripple in the bandpass regions can help mitigate a visible color change at lower or higher temperatures. This design trick was also shown to work in the OIC 2013 Design Contest [6] where there was a need to maintain the color green of a mirror from angles going from normal incidence to  $60^{\circ}$ .

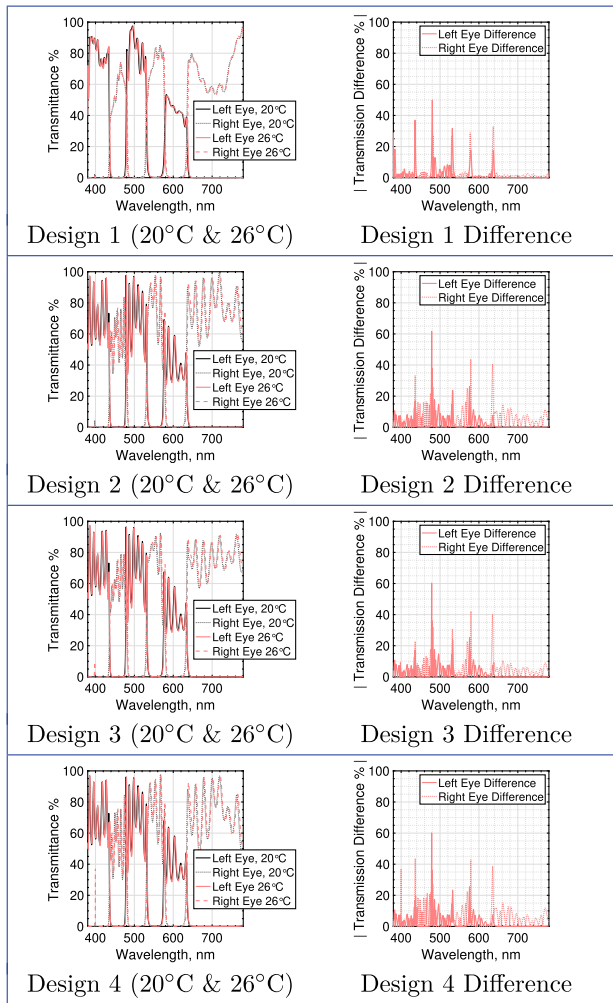


**Fig. 14.** Design comparison for 20°C and 26°C for designs 1–4. Left column compares projector and outdoor filter performance, and right column compares the differences in performance.

#### 4. CONCLUSION

Black box design Problem A demonstrated how difficult is the reconstruction of a design using spectral measurements of the reflectance and transmittance without any additional *a priori* information. Only one designer, Lemarchand, was able to find the solutions. In fact, some additional information was provided: we specified a chemical composition of the coatings, and the selection of the refractive indices was limited by a rather wide, but discrete, set of complex refractive indices. Also contest rules limited the number of layers in submitted designs by 35 and 75, and these restrictions gave some hint on possible design complexity.

Lemarchand started with the estimation of layer number in the designs, and this strategy was very successful. Tonova also used an initial search with only two materials to find a rough initial starting design, and this approach allowed her to find solutions with low additional metrics  $\Delta_n$  and  $\Delta_k$ . She limited the search to a narrow subset of materials in the succeeding steps, and this did not allow her to improve the design further. In any case, employing any additional hypothesis on the possible

design structure at the initial stage of designing appeared to be a very successful strategy.

The Black Box Design Challenge was performed in a very idealistic case, when measurements were provided without any measurement errors. In practice, measurement errors are unavoidable, and they are one of the main factors affecting the performance of all reverse-engineering methods. We cite a message from Southwell [7]:

*In the Problem Statement you ask, “Is it possible to reconstruct the exact theoretical design structure using reverse engineering of measured spectra?” The results of the contest indicates the answer is yes because one did it. But that was done with perfect error-free data. Otherwise, I claim, that it would not be possible with real typical measurement error. The fact that our entry got very good fits, (very low merit functions) using more layers which increases the degrees of freedom, indicates that the extra layers can fit the spectra very well. The true solution may be lost in the noise. Thus, I believe that the design contest shows that the answer to your question is probably, “No,” you cannot extract the exact layer structure in the presence of measurement noise.*

We can only agree with this statement, and we are happy that the Black Box Challenge demonstrated all complexity of the reverse engineering and the necessity of *a priori* information for success.

The design challenges posed in Problem B were constructed based on COVID-19 lockdown experiences in 2020. An outdoor cinema was a way to entertain large groups of people, especially friends and family, where there was enough room for social distancing. For 3D cinema, eyewear is a crucial component used to produce the effect. Problem B required the same multi-bandpass filters for the projector and the eyewear. However, the outdoor environment caused temperature differences between the filters in the projector and those worn on the user. The designs for each filter needed to mitigate the changes in transmitted color due to a relatively cold or hot outdoor temperature.

Ruiz submitted four designs, where each were optimized for a different outdoor temperature range. The winning designs for both cold and hot environments were not typical multi-bandpass filters. For most bandpass filters, the transmission region is smooth and even, whereas Ruiz’s designs had significant fluctuations or noise in the bandpass regions. CIELAB lightness ( $L^*$ ) was high for the filters despite the high frequency transmission changes in each wavelength band. The noise produced a color-balance compensation for both the filter’s blueshift in a cold environment and a redshift in a hot environment, such that the color difference was minimized between the projector and eyewear filters. This compensation strategy is also very effective for angle of incidence changes [7].

Only a few of the designers mentioned the design software that was used. Lemarchand and Tonova used OptiLayer, and Bolshakov used Filmstar. Other designers used their own custom code or did not mention the software used. The winning designs for the OIC 2022 Design Contest were based on the lowest MFs achieved. It has been reiterated over many years that we have offered a design challenge at OIC in which in the real world a low MF does not necessarily mean the best overall design. Many of the best designs come from designers that start

with a plan of action or strategy, and not just hitting the *optimize* button in any design software.

**Acknowledgment.** The OIC Design Contest Committee thank all of the designers for submitting such wonderful and insightful designs and thank the Optica and the OIC Technical Committee for hosting this contest in 2022.

**Disclosures.** The authors declare no conflicts of interest.

**Data availability.** Data underlying the results presented in this paper can be found in [Data File 1](#), Ref. [2], [Data File 3](#), Ref. [3], [Data File 2](#), Ref. [8], [Data File 4](#), Ref. [9].

**Supplemental document.** See [Supplement 1](#) for supporting content.

## REFERENCES

1. T. Amotchkina, M. Trubetskov, V. Pervak, and A. Tikhonravov, "Design, production, and reverse engineering of two-octave antireflection coatings," *Appl. Opt.* **50**, 6468–6475 (2011).
2. M. Trubetskov, "Data File 1—AR virtual spectrophotometer measurements," figshare, 2022, <https://doi.org/10.6084/m9.figshare.21733232>.
3. M. Trubetskov, "Data File 3—NPSWP virtual spectrophotometer measurements," figshare, 2022, <https://doi.org/10.6084/m9.figshare.21733238>.
4. "Useful color data," 2021, <https://www.rit.edu/science/munsell-color-science-lab-educational-resources>.
5. J. Ruiz (personal communication, 2022).
6. K. Hendrix, J. D. T. Kruschwitz, and J. Keck, "Optical Interference Coatings Design Contest 2013: angle-independent color mirror and shortwave infrared/midwave infrared dichroic beam splitter," *Appl. Opt.* **53**, A360–A376 (2014).
7. B. Southwell (personal communication, 2022).
8. M. Trubetskov, "Data File 2—AR design," figshare, 2022, <https://doi.org/10.6084/m9.figshare.21733235>.
9. M. Trubetskov, "Data File 4—NPSWP design," figshare, 2022, <https://doi.org/10.6084/m9.figshare.21733241>.